Apelin protects against abdominal aortic aneurysm and the therapeutic role of neutral endopeptidase resistant apelin analogs

Wang Wang[a,b,c], Mengcheng Shen[b,c], Conrad Fischer[d], Ratnadeep Basu[a,b], Saugata Hazra[e,f], Pierre Couvineau[g], Manish Paul[h], Faqi Wang[a,b], Sandra Toth[i], Doran S. Mix[i], Marko Poglitsch[j], Norma P. Gerard[k], Michel Bouvier[g], John C. Vederas[d], Josef M. Penninger[l], Zamaneh Kassiri[b,c], and Gavin Y. Oudit[a,b,c,1]

[a]Division of Cardiology, Department of Medicine, University of Alberta, Edmonton, AB T6G 2G3, Canada; [b]Mazankowski Alberta Heart Institute, University of Alberta, Edmonton, AB T6G 2J2, Canada; [c]Department of Physiology, University of Alberta, Edmonton, AB T6G 2R7, Canada; [d]Department of Chemistry, University of Alberta, Edmonton, AB T6G 2N4, Canada; [e]Department of Biotechnology, Indian Institute of Technology, 247667 Roorkee, Uttarakhand, India; [f]Centre for Nanotechnology, Indian Institute of Technology, 247667 Roorkee, Uttarakhand, India; [g]Department of Biochemistry and Molecular Medicine, Faculty of Medicine, University of Montreal, Montreal, QC H3C 3J7, Canada; [h]Department of Biotechnology, North Orissa University, 757003 Baripada, Odisha, India; [i]Division of Vascular Surgery, University of Rochester, Rochester, NY 14642; [j]Attoquant Diagnostics, 1030 Vienna, Austria; [k]Boston Children's Hospital, Beth Israel Deaconess Medical Center, Harvard Medical School, Boston, MA 02115; and [l]Department of Medical Genetics, Life Sciences Institute, University of British Columbia, Vancouver, BC V6H 3N1, Canada

Edited by Christine E. Seidman, Howard Hughes Medical Institute, Brigham and Women's Hospital, Harvard Medical School, Boston, MA, and approved May 21, 2019 (received for review January 7, 2019)

Abdominal aortic aneurysm (AAA) remains the second most frequent vascular disease with high mortality but has no approved medical therapy. We investigated the direct role of apelin (APLN) in AAA and identified a unique approach to enhance APLN action as a therapeutic intervention for this disease. Loss of APLN potentiated angiotensin II (Ang II)-induced AAA formation, aortic rupture, and reduced survival. Formation of AAA was driven by increased smooth muscle cell (SMC) apoptosis and oxidative stress in *Apln*$^{-/y}$ aorta and in APLN-deficient cultured murine and human aortic SMCs. Ang II-induced myogenic response and hypertension were greater in *Apln*$^{-/y}$ mice, however, an equivalent hypertension induced by phenylephrine, an α-adrenergic agonist, did not cause AAA or rupture in *Apln*$^{-/y}$ mice. We further identified Ang converting enzyme 2 (ACE2), the major negative regulator of the renin-Ang system (RAS), as an important target of APLN action in the vasculature. Using a combination of genetic, pharmacological, and modeling approaches, we identified neutral endopeptidase (NEP) that is up-regulated in human AAA tissue as a major enzyme that metabolizes and inactivates APLN-17 peptide. We designed and synthesized a potent APLN-17 analog, APLN-NMeLeu9-A2, that is resistant to NEP cleavage. This stable APLN analog ameliorated Ang II-mediated adverse aortic remodeling and AAA formation in an established model of AAA, high-fat diet (HFD) in *Ldlr*$^{-/-}$ mice. Our findings define a critical role of APLN in AAA formation through induction of ACE2 and protection of vascular SMCs, whereas stable APLN analogs provide an effective therapy for vascular diseases.

apelin | ACE2 | neutral endopeptidase | aneurysm | angiotensin II

AAA is defined as an enlargement of the AA to >1.5-fold of its normal size, and the overall AAA prevalence is estimated to be 6% in men and 1.6% in women (1–3). The asymptomatic nature of AAA makes the diagnosis extremely challenging, whereas ruptured AAA accounts for ∼15,000 deaths in the United States annually (4). Open surgical repair or endovascular repair are the only treatment options for patients with advanced AAA. Importantly, several modes of medical therapy have failed to provide benefits in patients with AAAs (1–3). Therefore, a better understanding of the cellular dysregulation and signaling networks responsible for the formation and progression of AAA is necessary for the discovery of novel and effective therapies.

Homeostasis of endothelial cells and vascular SMCs (VSMCs), the major cell populations of the vascular wall, play a crucial role in AAA development and disease progression. Activation of the RAS and production of Ang II lead to adverse vascular remodeling as well as many other cardiovascular pathologies (5). Meanwhile, the APLN pathway has emerged as a major peptide hormone pathway capable of exerting beneficial metabolic and cardiovascular effects (6–10). APLN is widely expressed in mammals including in endothelial cells and VSMCs (11, 12). The APLN precursor peptide is processed into several peptides including APLN-17 (13, 14), the most potent APLN peptide in the cardiovascular system. ACE2 is the major negative regulator of the RAS and converts Ang II into the vasculoprotective peptide, Ang 1–7 (5, 15–17).

In this study, we defined a marked susceptibility of the abdominal aorta lacking APLN to the development of AAA in response to Ang II. This was driven by reduced ACE2 levels, deficiency, oxidative stress, and apoptotic cell death of VSMCs. We identified NEP as a key enzyme that degrades and inactivates the active APLN-17 peptide, developed a stable APLN-17 analog resistant to NEP degradation, and established the

Significance

Vascular diseases remain a major health burden, and AAAs lack effective medical therapy. We demonstrate a seminal role for APLN in AAA pathogenesis based on loss-of-function and gain-of-function approaches and included human vascular SMCs and AA tissue obtained from patients. We identified NEP as a dominant inactivating enzyme for native APLN-17. This allowed us to design and synthesize a stable and bioactive APLN analog resistant to NEP degradation that showed profound therapeutic effects against AAA. Our study clearly defines the APLN pathway as a central node in the pathogenesis of AAA and elucidate a therapeutic strategy of enhancing the APLN pathway by using a stable APLN analog to treat AAA.

Author contributions: W.W., J.C.V., Z.K., and G.Y.O. designed research; W.W., M.S., C.F., S.H., P.C., M. Paul, F.W., M. Poglitsch, M.B., and G.Y.O. performed research; W.W., C.F., S.T., D.S.M., N.P.G., J.C.V., and J.M.P. contributed new reagents/analytic tools; W.W., M.S., C.F., R.B., S.H., P.C., M. Paul, F.W., S.T., D.S.M., M. Poglitsch, M.B., Z.K., and G.Y.O. analyzed data; and W.W. and G.Y.O. wrote the paper.

Conflict of interest statement: Our apelin analogs have been submitted for patenting.

This article is a PNAS Direct Submission.

[1]To whom correspondence may be addressed. Email: gavin.oudit@ualberta.ca.

This article contains supporting information online at www.pnas.org/lookup/suppl/doi:10.1073/pnas.1900152116/-/DCSupplemental.

Published online June 12, 2019.

therapeutic effects of this developed stable APLN analog in preventing vascular disease and formation of AAA.

Results

Loss of APLN Enhances Susceptibility to AAA. Histological analyses of human AAA revealed severely disrupted medial structure characterized by fragmented elastin fibers associated with the loss of SMCs and increased cell death in AAA specimens compared with the nondiseased aorta (NDA) (Fig. 1 *A* and *B* and *SI Appendix*, Fig. S1*A* and Table S1). These structural changes in the aneurysmal aorta were associated with increased APLN levels compared with nonaneurysmal aorta (Fig. 1 *C* and *D* and *SI Appendix*, Fig. S1*B*) and APLN was increased in Ang II-infused wild-type (WT) (*Apln*$^{+/y}$) mice aorta (Fig. 1 *E* and *F*). A similar pattern was also seen in the thoracic aorta from patients with bicuspid aortic valve and aortopathy (*SI Appendix*, Fig. S2*A*).

Ang II is a well-known mediator of adverse vascular remodeling and is widely used in AAA models (18–21). The up-regulation of APLN levels in the diseased aorta suggest that the APLN pathway is responsive to disease. To determine the role of APLN in AAA, we tested the effects of Ang II in WT (*Apln*$^{+/y}$) and APLN knockout (*Apln*$^{-/y}$) mice. Four weeks of Ang II infusion resulted in high incidence of severe AAA in the *Apln*$^{-/y}$ but not in parallel WT mice (Fig. 2*A*). The AAA in *Apln*$^{-/y}$ mice was associated with aortic dissection, intramural hematoma, and increased mortality due to aortic rupture (Fig. 2 *B* and *C*). Among the 23 *Apln*$^{-/y}$ mice that received Ang II, 5 died from AAA rupture, 18 survived, and 12 of the survivors developed AAA (Fig. 2 *A*–*C*). Vascular ultrasound imaging showed progressive greater dilation, localized aneurysm formation, and decreased compliance (aortic expansion index) in the abdominal aorta of Ang II-infused *Apln*$^{-/y}$ compared with *Apln*$^{+/y}$ mice, whereas no difference was observed between the genotypes at baseline (Fig. 2*D*). Consistent with the phenotypic changes in the abdominal aorta, thoracic aorta also displayed adverse remodeling in *Apln*$^{-/y}$ compared with *Apln*$^{+/y}$ mice (*SI Appendix*, Fig. S2*B*). Histological analyses confirmed disruption of the elastin lamellae in the aortic media and excess fibrotic deposition in the adventitia in *Apln*$^{-/y}$ mice compared with the uniform thickening of the aortic wall in *Apln*$^{+/y}$ mice in response to Ang II (Fig. 2*E*). Overall, our findings demonstrate that APLN is a major determinant in the pathogenesis of AAA.

APLN Deficiency Promotes Ang II-Induced Hypertension and VSMC Stress. We next explored the mechanism for the enhanced susceptibility of APLN-deficient mice to Ang II-induced AAA. We

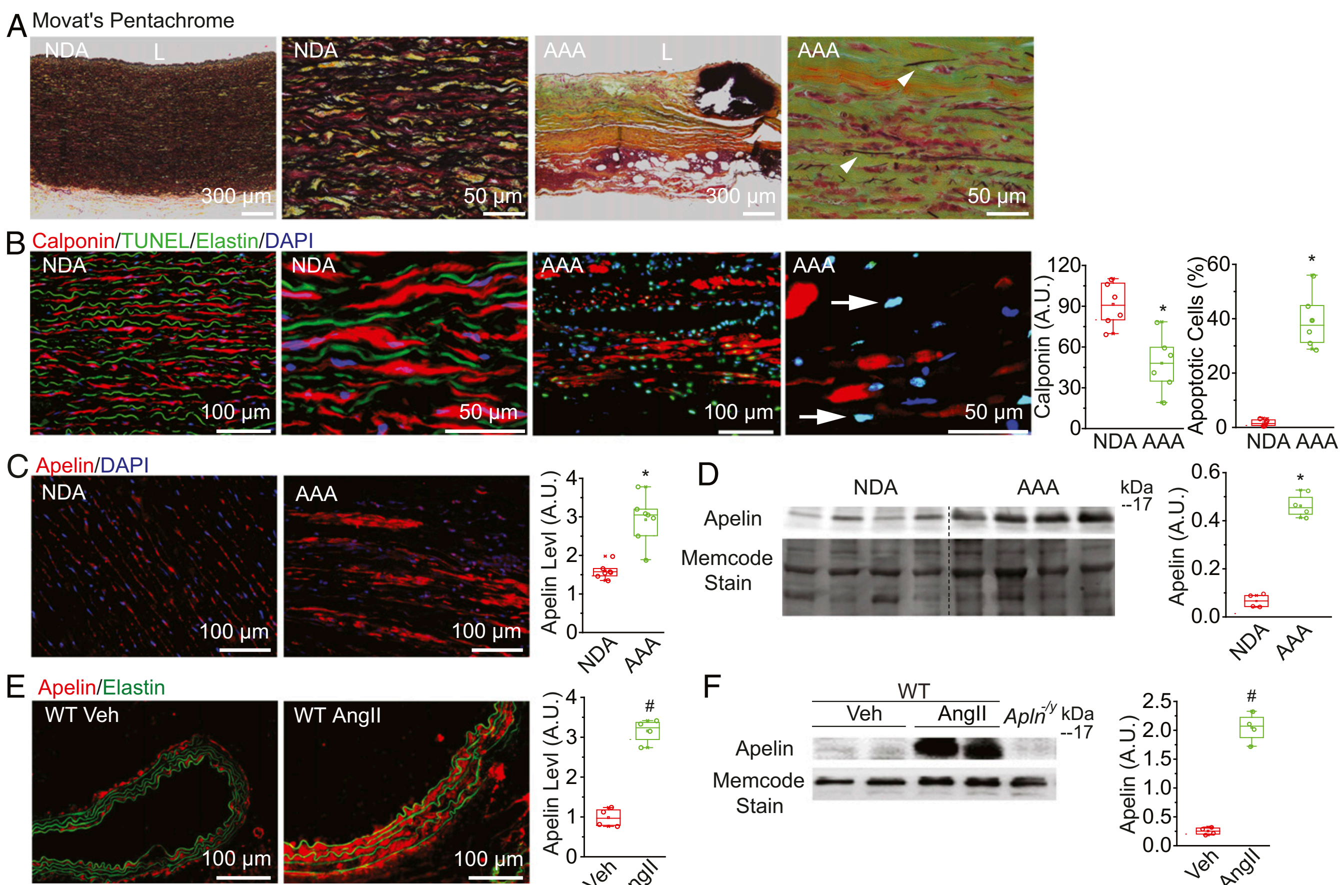

Fig. 1. Up-regulation of APLN levels in vascular disease. (*A* and *B*) Adverse structural remodeling in surgical resected AAA specimens from patients as revealed by Movat's pentachrome (*A*) and anti-calponin staining to visualize SMCs (red, *B*) of NDA and AAA. The arrow heads in AAA images point to elastin fiber fragments. L = aortic lumen. (*B*) Elastin fiber autofluorescence appears green. DAPI staining (blue) was used to visualize the nuclei. Averaged SMC content (calponin-positive staining), and apoptotic SMCs (positive for TUNEL in green and DAPI staining) in the NDA and AAA are shown as boxes with scatter plots on the right. n = 6/group. The arrows in AAA images point to apoptotic cells. (*C*) Immunostaining for APLN (red) with DAPI nuclear staining (blue), and Western blots for APLN (*D*) in NDA and AAA specimens with averaged quantification of APLN levels shown in boxes with scatter plots; n = 7/group in *C*, n = 4/group in *D*. (*E*) Immunostaining for APLN (red) with DAPI nuclear staining (blue), and Western blots (*F*) in abdominal aorta from WT mice receiving saline as vehicle (Veh) or Ang II for 4 wk (1.5 mg/kg/d) with averaged quantification of APLN levels shown in boxes and scatter plots; n = 4/group. *$P < 0.05$ compared with the NDA group; $^{\#}P < 0.05$ compared with the Veh group; A.U., arbitrary units.

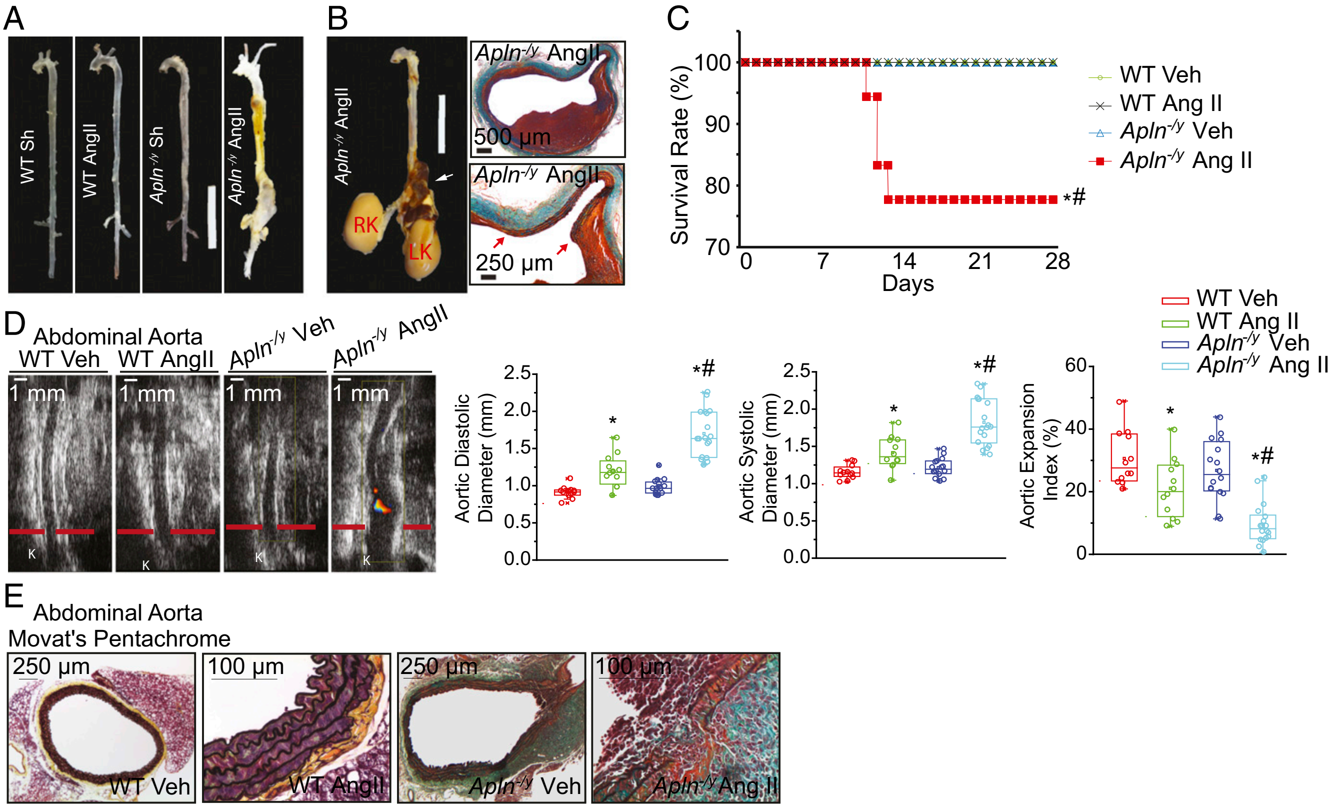

Fig. 2. APLN deficiency increases susceptibility to AAA and vascular SMC death. (*A* and *B*) Representative pictures of the whole aorta from all groups showing the presence of aneurysms (*A*), aortic dissection, and rupture (*B*) leading to hemorrhage in the peritoneal cavity in the *Apln*$^{-/y}$-Ang II group. The white arrow points to a hemorrhage. RK = right kidney, LK = left kidney, and the red arrows point to ruptured ends of elastin lamellae. (*C*) Kaplan Meir survival curve showing mortality due to aortic rupture assessed by logarithm-rank testing. n = 12–18/group. (*D*) Ultrasonographic B-mode images of the AA in Ang II-infused WT and *Apln*$^{-/y}$ mice. "*K*" indicates the top of the left kidney as a reference, and the *red lines* show where measurements of aortic diameter were obtained (suprarenal). Averaged aortic systolic and diastolic diameters and aortic systolic expansion index of AA in vehicle- or Ang II-infused groups are shown. n = 12–18/group. (*E*) Histological analysis (Movat's pentachrome staining) showing disruption of the elastin lamellae in the medial aortic wall with fibrotic deposition in *Apln*$^{-/y}$ mice compared with the uniform thickening of the aortic wall in WT mice exposed to Ang II. $^{*}P < 0.05$ compared with the Veh group; $^{\#}P < 0.05$ compared with the WT-Ang II group.

determined the impact of *Apln* deficiency on vascular function and showed stronger Ang II-induced vasoconstriction in *Apln*$^{-/y}$ mesenteric resistance arteries compared with *Apln*$^{+/y}$ arteries associated with marked suppression of basal phospho-eNOS (Ser1177) levels (Fig. 3*A* and *SI Appendix*, Fig. S3 *A* and *B*). In vivo telemetric blood pressure measurement demonstrated that, although baseline blood pressure was equivalent in both genotypes, Ang II resulted in a greater increase in mean arterial blood pressure (MABP) during the day and night in *Apln*$^{-/y}$ compared with parallel *Apln*$^{+/y}$ mice (Fig. 3*B*). In contrast to Ang II effects, the intrinsic myogenic response and maximal vasoconstriction in response to high extracellular potassium was equivalent in both genotypes (*SI Appendix*, Fig. S3 *C–E*). To test whether the Ang II-induced higher blood pressure in *Apln*$^{-/y}$ mice accounted for AAA formation, we used another hypertensive agent, phenylephrine (PE), to induce the same degree of hypertension. Interestingly, no AAA was observed in either *Apln*$^{-/y}$ mice or their parallel control *Apln*$^{+/y}$ mice after 4 wk of PE infusion (*SI Appendix*, Fig. S4). These results demonstrate that the APLN-deficient vasculature is intrinsically susceptible to the adverse effects of Ang II-induced vascular remodeling.

We investigated the cellular basis for the enhanced susceptibility to AAA formation in *Apln*$^{-/y}$ mice and found reduced VSMC density, increased apoptotic cell death, and cleaved caspase 3 levels following 2 wk (*SI Appendix*, Fig. S5*A*) and 4 wk of Ang II infusion (Fig. 3 *C* and *D*). These cellular phenotypes were concordant with a marked suppression of survival signaling pathways, Akt and Erk1/2 pathways, whereas preventing Ang II-mediated phosphorylation of p38 and JNK1/2 MAPK (*SI Appendix*, Fig. S6). These changes were associated with elevated oxidative stress as evident by the increased number of dihydroethidium (DHE)-positive cells in the aortic wall coupled with elevated NADPH oxidase (Fig. 3 *E* and *F* and *SI Appendix*, Fig. S5*B*) and in situ gelatinase activities reflecting the action of matrix metalloproteinases 2 and 9 (*SI Appendix*, Fig. S7).

Next, we characterized the impact of APLN deficiency on VSMCs in response to Ang II in vitro. In cultured primary aortic SMCs from human and mouse aorta (*SI Appendix*, Fig. S8), APLN expression was knocked down using specific APLN-siRNA (siAPLN), whereas scrambled siRNA (siNS) was used as the control (Fig. 4*A*). Ang II treatment increased *Apln* mRNA levels in control human and mouse SMCs (siNS) but induced a markedly higher rate of apoptotic cell death in the siAPLN SMCs of both species (Fig. 4*B*) accompanied by elevated oxidative stress and DHE levels in these SMCs (Fig. 4*C*). ACE2 has emerged as a major negative regulator of the RAS by converting Ang II into Ang 1–7 (5). We identified Ang II-mediated transcriptional up-regulation of *Ace2* mRNA in human and murine VSMCs (Fig. 4*D*) in association with increased ACE2 protein levels in diseased murine aortas (Fig. 4 *E* and *F*). Suppression of APLN markedly inhibited Ang II-mediated rise in *Ace2* mRNA and ACE2 levels (Fig. 4 *D–F*). These data demonstrate that Ang II-induced AAA in *Apln*$^{-/y}$ mice is due to the intrinsic susceptibility of the vasculature to adverse remodeling due to the lack

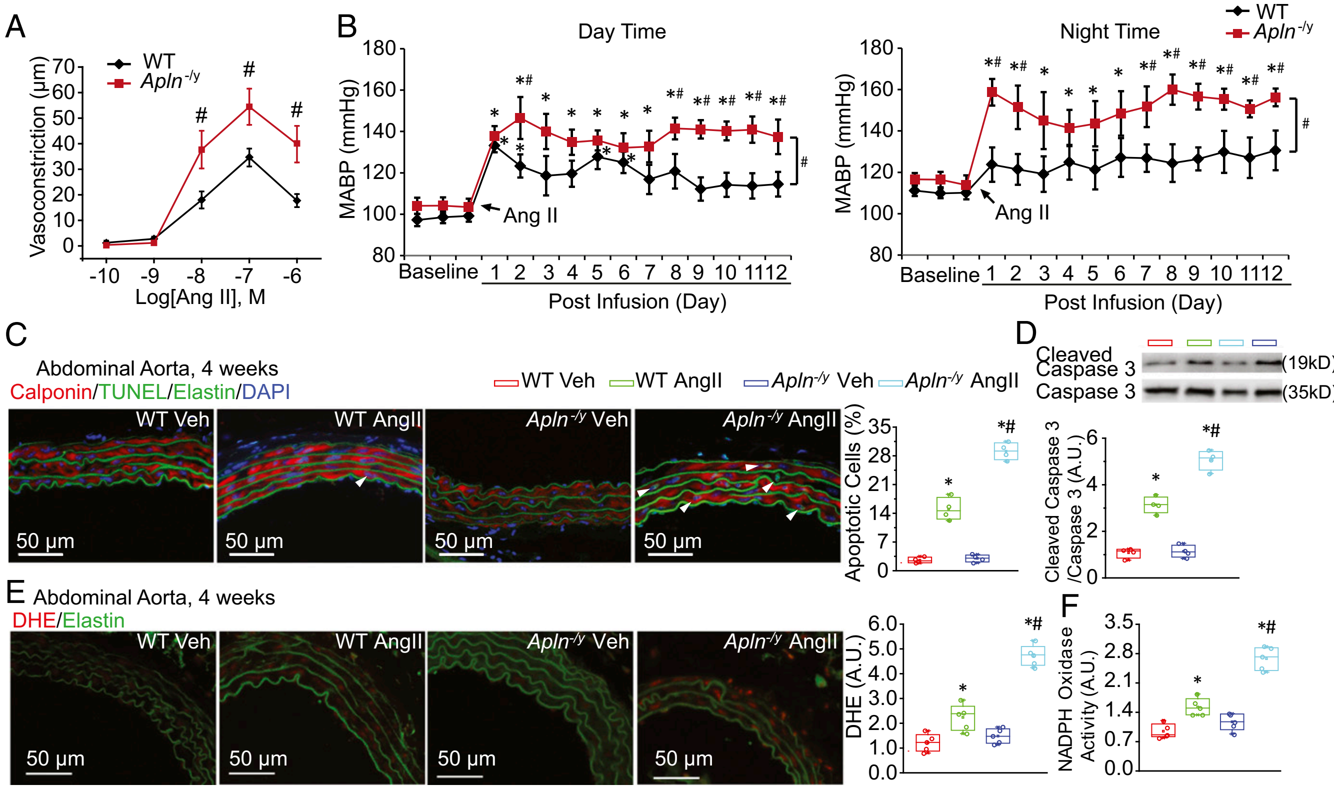

Fig. 3. Loss of APLN sensitizes the vasculature and vascular SMCs to the pathological effects of Ang II. (*A*) Myogenic vasoconstrictor response to Ang II using pressure myography and third-order mesenteric arteries in WT and *Apln*$^{-/y}$ vessels; *n* = 8/group. (*B*) Telemetry blood pressure recording in WT and *Apln*$^{-/y}$ mice before and over 2 wk of Ang II infusion (1.5 mg/kg/d); MABP; *n* = 8/group. The arrows indicate when Ang II infusion starts. (*C*) Immunostaining for SMCs (calponin, red), apoptosis (TUNEL, green), nuclear DAPI staining (blue), and elastin fiber autofluorescence (green) in AA. Averaged percentage of apoptotic cells in each group is shown in the boxes with scatter plots; *n* = 4/group/genotype. (*D*) Western blot assay for total and cleaved caspase 3 and averaged cleaved-to-total caspase 3 levels is shown as a box with a scatter plot; *n* = 4/group. (*E*) DHE-based fluorescence in the abdominal aortic wall with (*F*) NADPH oxidase activity (*n* = 5/group/genotype). *$P < 0.05$ compared with the Veh group; #$P < 0.05$ compared with the WT-Ang II group.

of APLN-mediated up-regulation of ACE2 and its prosurvival effects on VSMCs.

NEP Is a Key Enzyme that Inactivates APLN Peptides. Our results suggest that enhancing APLN action may be a therapeutic strategy for preventing or slowing the progression of AAA, a disease lacking effective medical therapy. We hypothesized that up-regulation of neutral endopeptidase (EC 3.4.24.11, NEP, and neprilysin) (22, 23) in disease degrades endogenous APLN thereby promoting AAA formation. Western blot analysis and immunostaining showed that NEP levels are increased in diseased murine and human aortas (Fig. 5 *A* and *B* and *SI Appendix*, Fig. S9). We next examined the ability of NEP in inactivating APLN peptides which could provide a fundamental mechanism for the pathogenesis of AAA. Computer modeling and simulation demonstrated a feasible model of APLN-17 binding with the active catalytic site in NEP (His583, His587, and Glu646) resulting in the cleavage of APLN-17 at 2 distinct sites, Arginine8-Lysine9 and Lysine9-Serine10 (Fig. 5*C* and *SI Appendix*, Fig. S10). Other active site residues in NEP that facilitate the binding of APLN-17 in the catalytic pocket are Arg102, Arg110, Glu533, Val541, Ser546, Ser547, Ile585, Glu646, Ile648, Gly655, Ala657, Tyr697, Val710, His711, and Arg717 (Fig. 5*C*). To confirm this prediction, we used a biochemical assay and found that ex vivo incubation of APLN-17 in human plasma with recombinant NEP resulted in efficient degradation of APLN whereas the application of a NEP inhibitor, sacubitrilat, elevated steady-state APLN levels (Fig. 6*A*) with corresponding inverse changes detected in plasma APLN 17 products, APLN 9–17 and APLN 10–17 peptides (*SI Appendix*, Fig. S11). The APLN degradation products were completely inactive demonstrating a key functional role of NEP in degrading APLN (Fig. 6*B*). We next tested the in vivo role of NEP in metabolizing APLN-17. Genetic loss or pharmacological inhibition (by sacubitrilat) of NEP potentiated the hypotensive action of APLN-17 (Fig. 6*C*) and markedly elevated plasma levels of APLN-17 (Fig. 6*D*). These results highlight a dominant role for NEP in metabolizing and inactivating the endogenous APLN-17 peptide, which implied the NEP resistant APLN analog is much needed for therapeutic use in vivo.

APLN Analogs Have Improve Pharmacokinetics and Equivalent Pharmacodynamics. Native APLN peptides are easily degraded and have short half-lives (14, 24, 25). Therefore, we designed and tested 35 different analogs and were able to identify and develop a long-lasting stable APLN-17 analog NMeLeu9Nle15Aib16BrPhe17-APLN-17 (abbreviated as APLN-NMeLeu9A2) (Fig. 7*A*) and confirmed a marked improvement in plasma levels and hypotensive effects (Fig. 7 *B* and *C*). The APLN receptor (formerly known as APJ) is the only known native receptor for APLN peptides in mammals (26). Binding studies with the murine APLN receptor showed that murine Gi activation and β-arrestin recruitment were maintained by APLN-NMeLeu9A2 at similar levels compared with native APLNs, minimizing the possibility of off-target effects of APLN analogs (Fig. 7 *D*–*G*). Our NEP resistant APLN-17 analog (APLN-NMeLeu9A2) represents a therapeutic approach for AAAs.

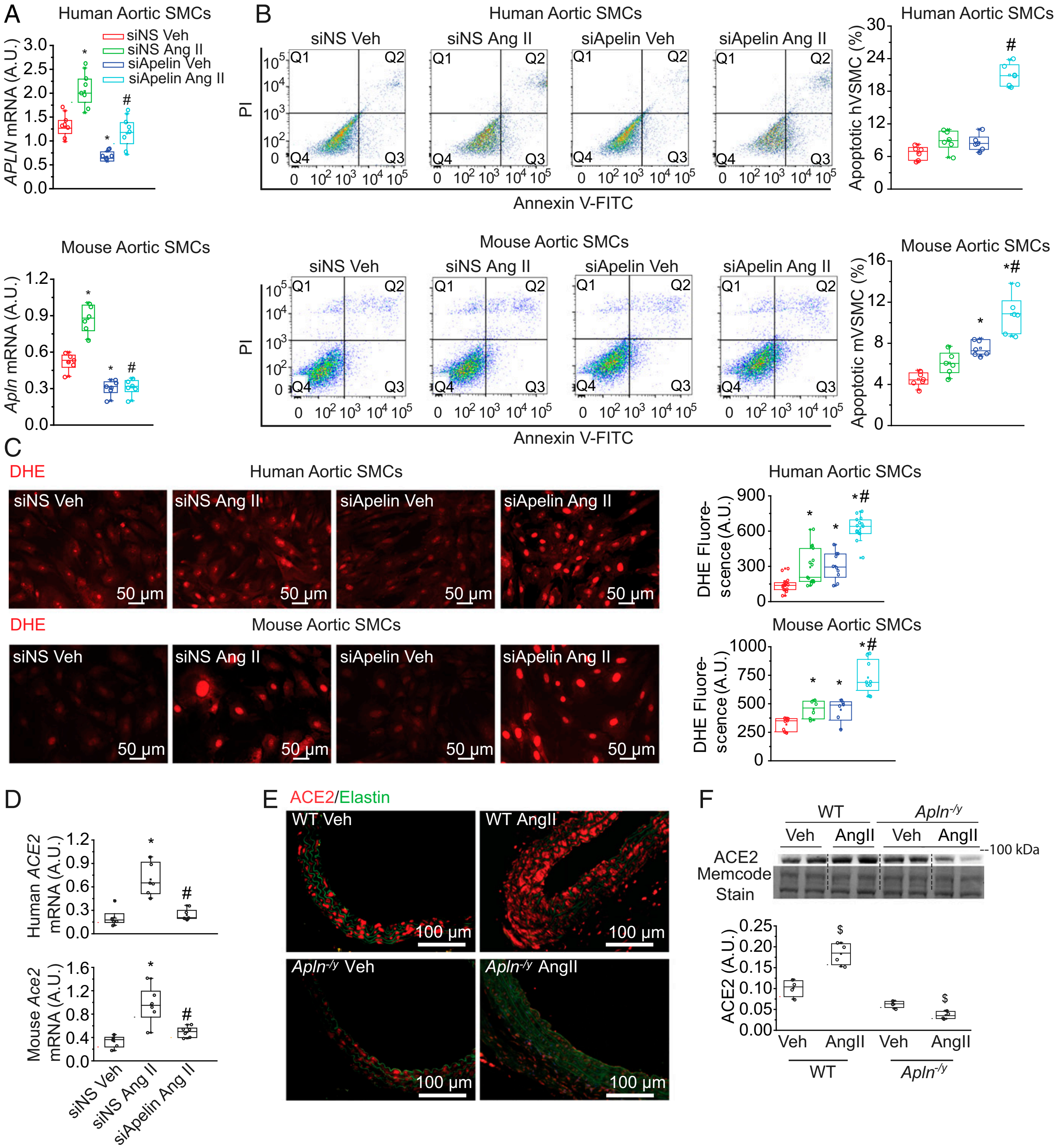

Fig. 4. Down-regulation of APLN expression in murine and human vascular SMCs increases Ang II-mediated cell death and oxidative stress. (*A*) siRNA treatment reduced *Apln* mRNA levels in human (*Upper*) and mouse (*Lower*) cultured primary aortic SMCs. (*B*) Flow cytometry analysis of cell death in human and mouse SMCs ± siNS or APLN-siRNA (siAPLN) treated with Ang II (10 μM) shows a marked increase in Ang II-induced cell death in APLN-deficient SMCs with quantitative analysis shown in the boxes and scatter plots; $n = 6$/group. (*C* and *D*) DHE-based fluorescence from cultured human and murine primary aortic SMCs (*C*) and *Ace2* mRNA expression (*D*) in response to siRNA targeting APLN expression ($n = 6$/group/genotype). (*E* and *F*) Representative immunostaining for ACE2 (red) and elastin fiber autofluorescence (green) (*E*) and Western blotting for ACE2 in WT and $Apln^{-/y}$ aorta (*F*) with averaged ACE2 levels shown as a box with a scatter plot; $n = 4$/group. $^{*}P < 0.05$ compared with the siNS + Veh group; $^{\#}P < 0.05$ compared with the siNS + Ang II group; $^{\$}P < 0.05$ compared with the corresponding Veh group. A.U., arbitrary units.

Therapeutic Effects of a Stable APLN Analog in an Experimental Model of AAA. To test the therapeutic potential of our synthetic APLN analog designed to be resistant to NEP-mediated degradation, we utilized a well-established model of an AAA. We used a murine model lacking low-density lipoprotein receptors ($Ldlr^{-/-}$) given a HFD and Ang II infusion (21, 27). Although the placebo-treated

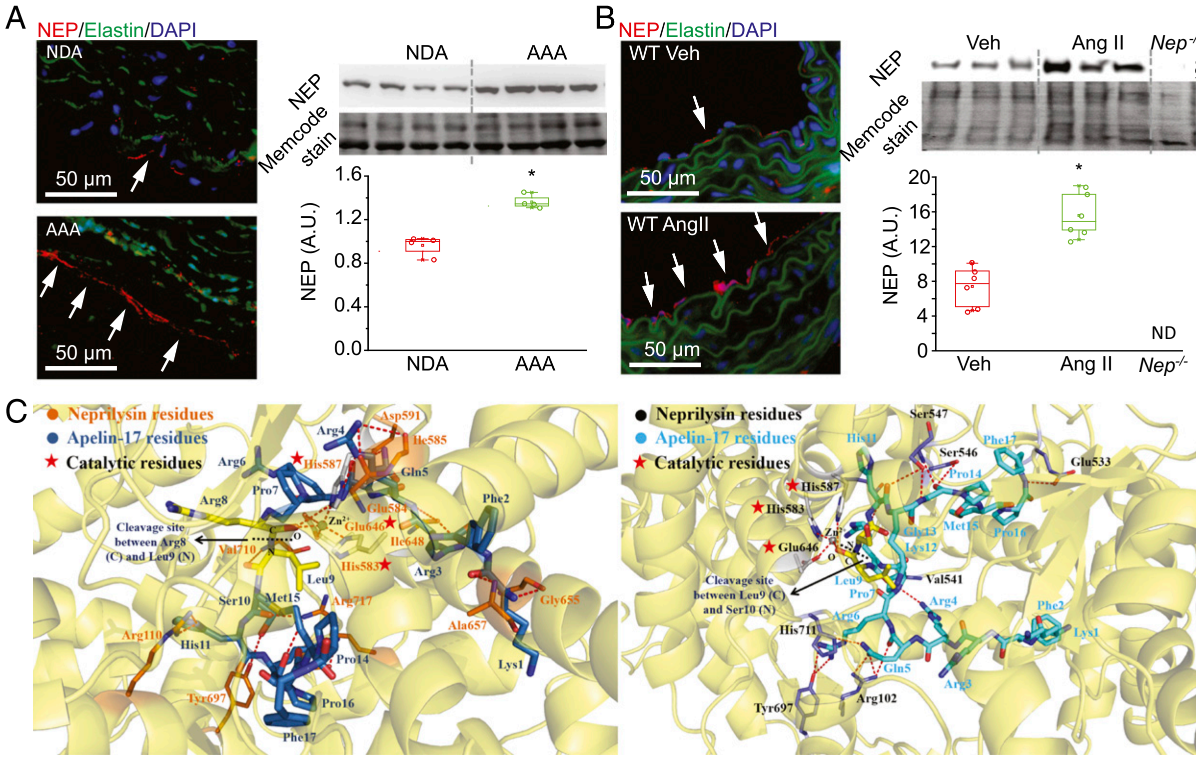

Fig. 5. NEP is up-regulated in the diseased aorta, and computer modeling predicts NEP mediates proteolytic cleavage of APLN-17. (*A* and *B*) Immunofluorescence staining and Western blot analysis of NEP in diseased human (*A*) and murine (*B*) aorta illustrating increased levels of NEP. $Nep^{-/-}$ aorta used as a negative control. ND, not detected; $n = 4$/group in (*A*), $n = 6$/group in *B*. (*C*) Computer-based in silico modeling showing the interaction between the catalytic site of NEP and cleavage sites in native APLN-17 peptide. $^{*}P < 0.05$ compared with the NDA or Veh group.

group ($Ldlr^{-/-}$-Ang II + placebo) showed a 50% mortality mainly due to aortic rupture in the abdominal region, treatment with the APLN analog ($Ldlr^{-/-}$-Ang II + APLN-NMeLeu9-A2) had no incidence of aortic rupture after 4 wk of Ang II infusion (Fig. 8*A*). Vascular ultrasound showed that the administration of APLN-NMe17A2 prevented aortic lumen dilation and preserved aortic

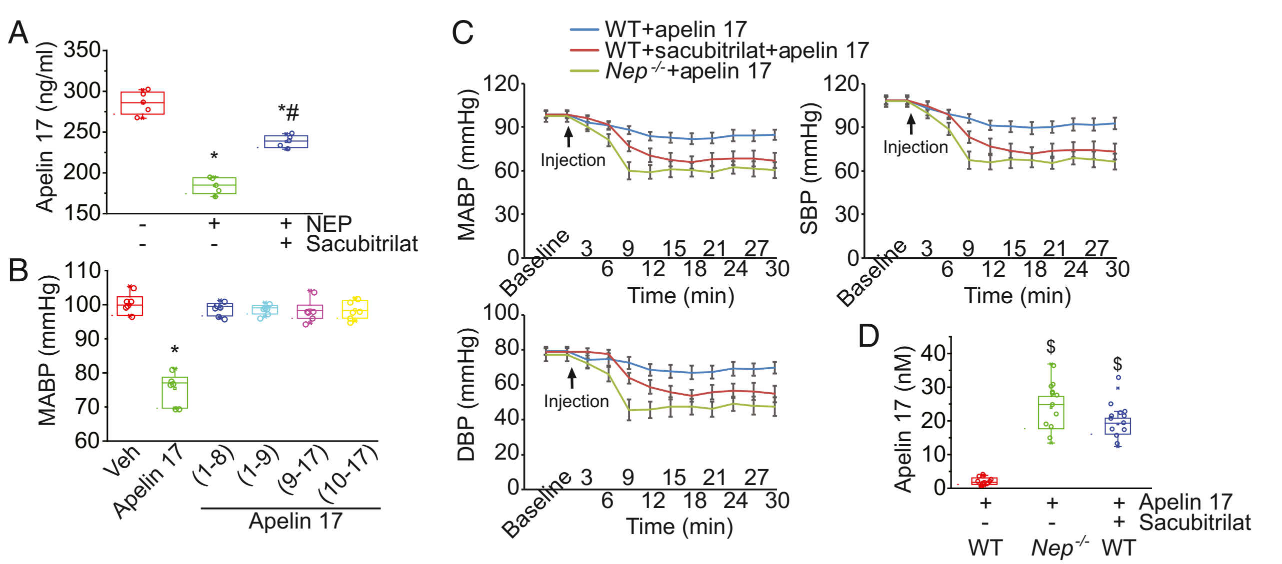

Fig. 6. NEP plays a key role in the inactivation of APLN-17: synthesis of NEP resistant APLN analogs. (*A* and *B*) In vitro assay using human plasma and human recombinant NEP demonstrating the ability of NEP to efficiently cleave APLN-17 (*A*) and in vivo blood pressure assay in WT mice demonstrating that the cleaved products of NEP action on APLN-17 peptides are inactive (*B*); NEPi = sacubitrilat; $n = 5$ to 6/group. (*C*) In vivo blood pressure assay in WT mice examining the vasodepressor activity of the NEP-mediated cleavage of the APLN-17 peptide product; $n = 6$/group; Averaged values represent mean ± SEM. MABP; SBP = systolic blood pressure; DBP = diastolic blood pressure. (*D*) Plasma APLN-17 levels in WT and $Nep^{-/-}$ mice and in response to pharmacological inhibition of NEP using sacubitrilat in WT mice; $n = 12$/group. $^{*}P < 0.05$ compared with the Veh group; $^{\#}P < 0.05$ compared with the NEP group without sacubitrilat; $^{\$}P < 0.05$ compared with the WT group without sacubitrilat.

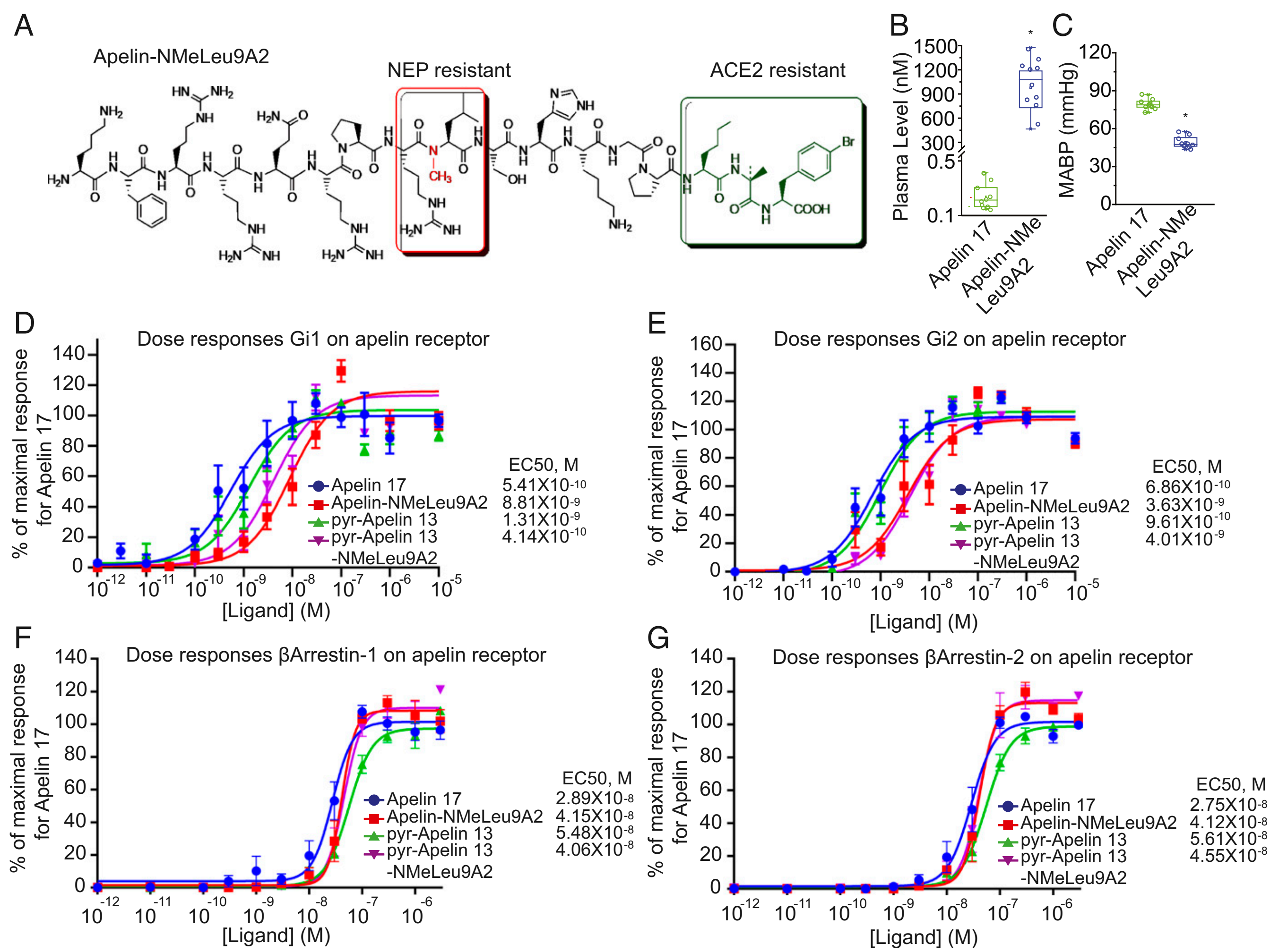

Fig. 7. APLN receptor coupled Gi activation and β-arrestin recruitment by APLN peptides and APLN analogs. (*A*–*C*) Schematic of the APLN-NMeLeu9A2 with plasma levels at 5 min posti.v. administration and blood pressure response compared with native APLN-17; $n = 10$/group. *$P < 0.05$ compared with the APLN 17 group. (*D*–*G*) Concentration-response effect of endogenous APLN peptides (K17F and pE13F) and metabolically stable APLN analogs (K17FA2 and pE13FA2) on murine (*D*) Gi1 activation, (*E*) Gi2 activation, (*F*) β–arrestin-1 recruitment, and (*G*) β–arrestin-2 recruitment. The data represent the mean ± the SEM of 4 to 8 independent experiments performed in duplicate. The data are expressed as percentages of the maximal response obtained for K17F. EC_{50} are listed on the right side of the concentration-response plots.

compliance (expansion index) (Fig. 8*B*). Structural analysis of the abdominal aorta provided definitive evidence that Ang II-mediated aortic pathology in *Ldlr*$^{-/-}$ mice was prevented by treatment with APLN-NMe17A2. Importantly, mice receiving APLN-NMeLeu9-A2 preserved SMC density and elastin structure, and reduced apoptosis (TUNEL and cleaved caspase 3 levels) in the aortic wall in response to 2 and 4 wk of Ang II infusion (Fig. 8 *C* and *D*). Intriguingly, APLN analog supplementation increased ACE2 levels in the aortic wall (Fig. 9 *A* and *B*), which has been reported to have vasculoprotective effects (15). In isolated VSMCs, Ang II-mediated production of reactive oxygen species determined by DHE fluorescence and NADPH oxidase activity were markedly attenuated by APLN-NMe17A2 (Fig. 9 *C* and *D*). Our results highlighted a dominant role of the APLN pathway in AAA and support the use of a stable APLN analog as a therapy for AAA (Fig. 9*E*).

Discussion

Vascular diseases remain a major health burden, and AAs lack effective medical therapy representing a progressive disease state with a life-threatening but unpredictable risk for rupture (1, 2). Currently, no pharmacological intervention effectively inhibits the progressive expansion of human AAAs or prevents aortic rupture (28, 29). In this study, we demonstrate a seminal role for APLN in AAA pathogenesis using loss-of-function and gain-of-function approaches. Using an Ang II-induced model of an AAA, loss of APLN resulted in greater adverse remodeling and propensity to develop an AAA, aortic rupture, and increased mortality. Given the short half-life of native APLN peptides, we identified NEP as a dominant inactivating enzyme for APLN-17. This allowed us to design and synthesize a stable and bioactive APLN analog that is resistant to NEP degradation, active in both blood pressure in vivo as well as in vitro APLN receptor binding studies; and it showed profound therapeutic effects for AAAs.

In aortic SMCs, APLN showed a dose-dependent protective effect against Ang II-induced apoptosis and reactive oxygen species stress, whereas loss of APLN exacerbated these responses, consistent with a dominant role of apoptotic loss of VSMCs in the progression of AAAs. A well-recognized characteristic in human AAAs is the increased abundance and activation of matrix metalloproteinases in the diseased aortic tissues that was modulated by the APLN pathway likely in response to changes in oxidative stress. APLN action on endothelial cells including promoting angiogenesis (6, 11, 12), APLN-mediated nitric oxide vasodilation

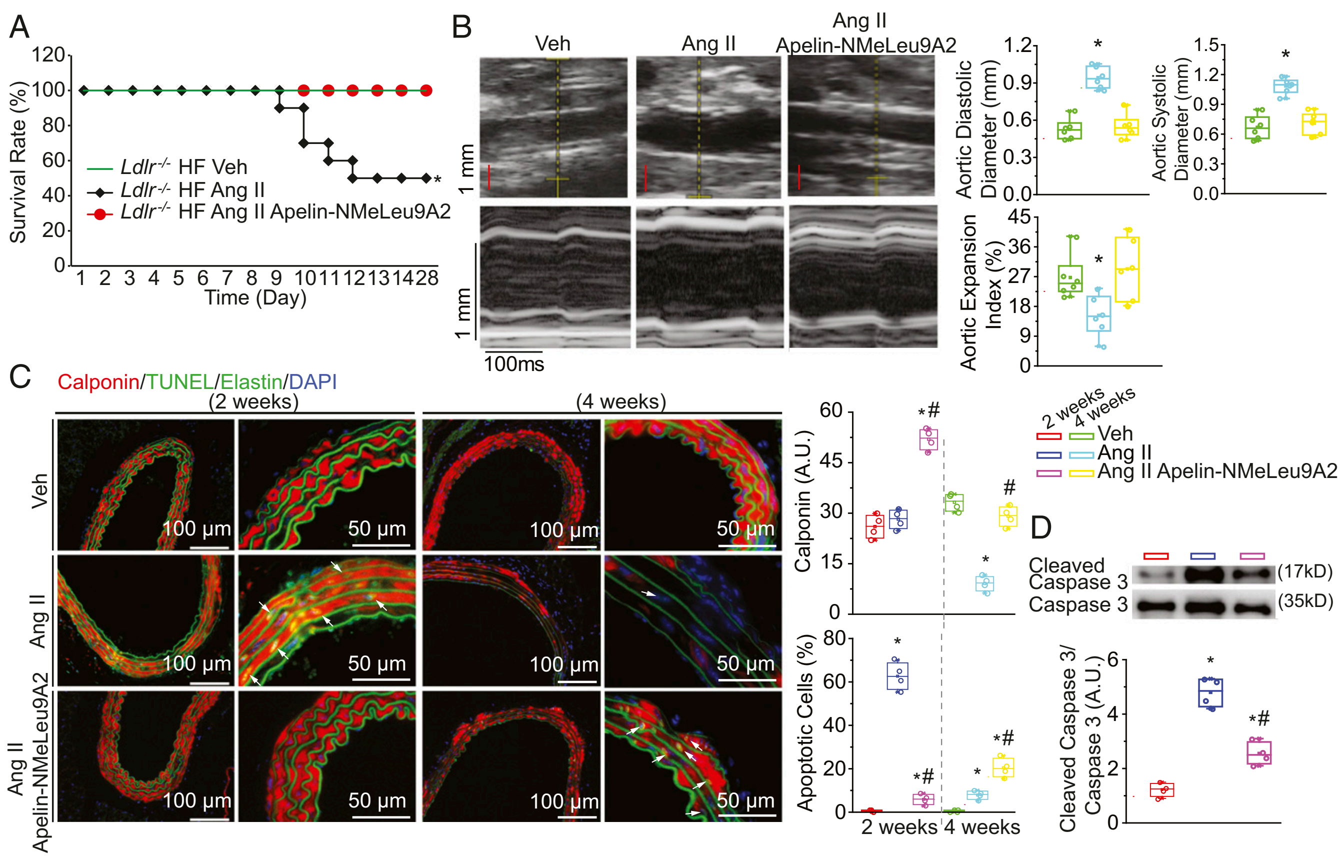

Fig. 8. NEP resistant APLN analog prevents Ang II-induced formation of AAA. (*A*) Survival curves showing the rate of mortality due to aortic rupture in *Ldlr*$^{-/-}$ mice on a HFD that received Veh (saline) or Ang II for 4 wk (1.5 mg/kg/d), or Ang II + APLN-NMeLeu9-A2. Mortality only presented in the HFD-Ang II group and is significantly higher than in other groups; $n = 15$/group. (*B*) Representative ultrasound images of the AA and averaged measurement for AA diameter during systole and diastole, and aortic expansion index, a measure of aortic wall compliance; $n = 6$/group. (*C*) Representative images of immunostaining for AA sections for calponin (SMC, red), TUNEL (green), DAPI (blue), and elastin fibers autofluorescence (green) in the indicated groups. Averaged quantification for calponin levels (measure of viable SMCs), and apoptotic cells (TUNEL positive) for each group is shown on the right; $n = 4$/group; arrows point to apoptotic cells. (*D*) Western blots for cleaved and total caspase 3 and averaged cleaved-to-total ratio for caspase 3; $n = 4$/group. $^*P < 0.05$ compared with the Veh group; $^\#P < 0.05$ compared with the Ang II group.

(11), and direct antagonism of the Ang II/Ang II type 1 receptor (10) highlights a key role of endothelial homeostasis as a critical pathway protecting the aorta from AAA formation (29). Ang II increases vascular tone, and excessive activation causes systemic hypertension, which is a major risk factor for AAA, atherosclerosis, and cardiac hypertrophy. The Ang II-induced vasoconstriction was potentiated in *Apln*$^{-/y}$ arteries without affecting passive elasticity and constrictive response to the α-adrenergic agonist PE. Indeed, Ang II-induced greater hypertension in *Apln*$^{-/y}$ mice compared with WT mice; however, this finding also poses a complexity in understanding the role of APLN in Ang II-induced adverse aortic remodeling because of the potential involvement of hypertension. As such, we used a PE-induced hypertension model and cultured murine and human aortic SMCs to demonstrate the specific susceptibility of APLN-deficient VSMCs to the pathological effects of Ang II.

Therapeutic supplementation with our stable APLN analog exhibited protective effects against AAA formation and up-regulated ACE2 which promotes vascular protective remodeling. Indeed, decreased ACE2 in the *Apln*$^{-/y}$ mesenteric artery could contribute to the increased sensibility of these mice to Ang II-induced AAA which highlights the vasculoprotective effect of Ang 1–7 (30). Basal ACE2 levels were lowered in the *Apln*$^{-/y}$ aorta compared with WT and failed to increase in response to Ang II. As such, the Ang II-mediated up-regulation of APLN in WT mice, which, in turn, up-regulates ACE2 leading to the conversion of Ang II into the protective Ang 1–7 peptide (5, 30) represents a critical negative feedback mechanism to confer vascular protection. The beneficial effects of APLN extend beyond the ACE2 pathway since Ang II infusion in *Ace2*$^{-/y}$ mice does not recapitulate the severe phenotype observed in the *Apln*$^{-/y}$ mice. Indeed, we identified a unique susceptibility of the APLN-deficient VSMCs to Ang II-mediated apoptotic cell death. *Apln*-deficiency reduced Ang II-mediated phosphorylation of Akt and Erk1/2 in the aorta consistent with the ability of the APLN peptide to activate a classic G protein coupled receptor leading to PI3 kinase activation and phosphorylation of Akt and Erk1/2 pathways (6, 14, 31).

Enhancing APLN action offers promising therapeutic effects on the aorta. We show that cleavage of APLN-17 by NEP completely inactivates this peptide, and the marked increase in NEP in a human aorta with AAA is likely a key mechanism of the progression of AAA. Computational modeling of the interaction between NEP and APLN-17 showed that the catalytic residues that promote the cleavage of the peptide, and other active site residues that assist APLN-17 binding are situated in the C-terminal region of the enzyme which implicate a domain specific enzyme catalysis. MICU2, a regulatory subunit of the mitochondrial calcium uniporter complex is protected from Ang II-mediated injury to the abdominal aorta associated with a marked up-regulation of *Apln* expression (20), whereas APLN also mediates protective effects in atherosclerosis (10) consistent

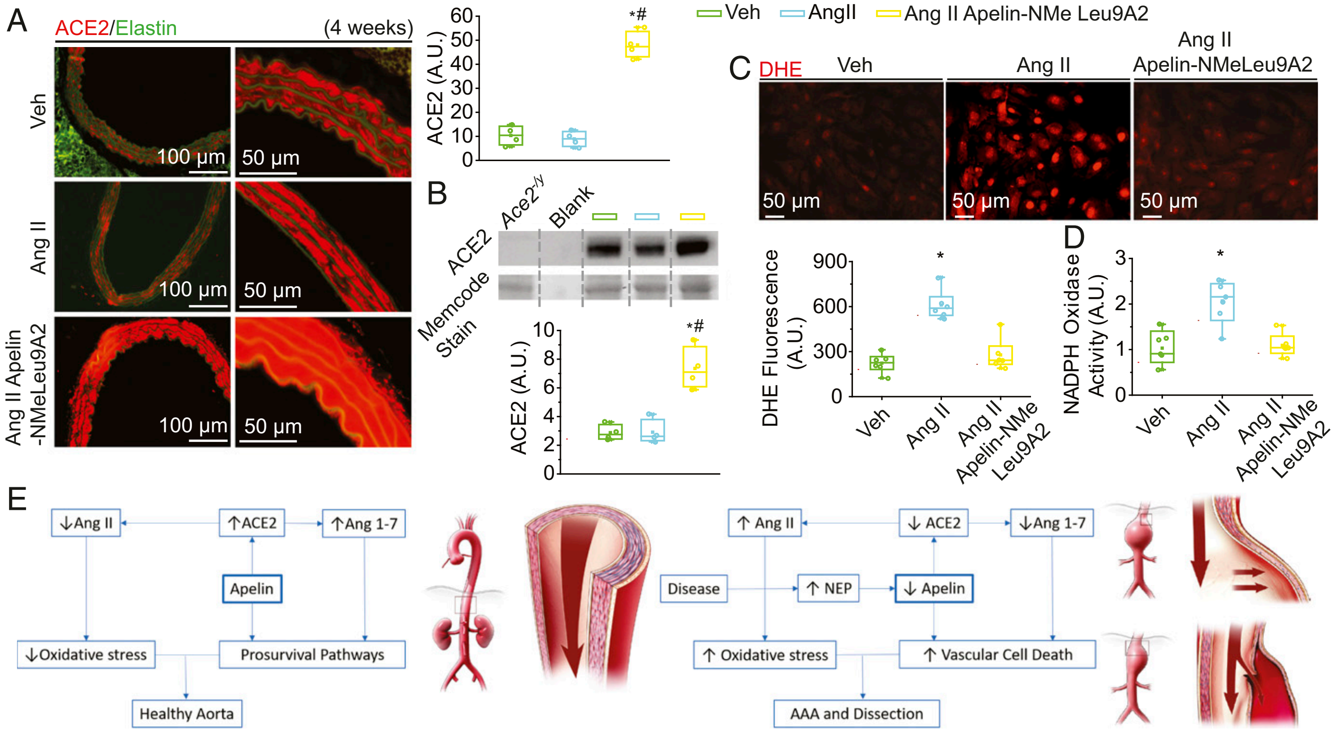

Fig. 9. Up-regulation of ACE2 by APLN analog: role of APLN in AAA pathogenesis. (*A*) Immunostaining for ACE2 and quantification in the AA of *Idlr*$^{-/-}$ on HFD receiving Veh, Ang II, or Ang II + APLN-NMeLeu9-A2; n = 4/group/genotype. (*B*) Western blots and quantification for ACE2 levels in abdominal aorta of *Idlr*$^{-/-}$ on HFD mice receiving Veh, Ang II + placebo, or Ang II + APLN-NMeLeu9-A2. Aortic proteins from *Ace2*$^{-/y}$ mice were used as a negative control; n = 4/group/genotype. (*C*) DHE-based fluorescence with (*D*) NADPH oxidase activity in cultured human primary aortic SMCs in response to Ang II and effects of APLN-NMeLeu9-A2; n = 6/group. (*E*) Schematic showing the interaction among APLN, ACE2, and NEP in a pathological setting driving the formation of AAA. *P < 0.05 compared with the placebo group. A.U., arbitrary units. Averaged values represent mean ± SEM.

with a vascular protective effect of APLN peptides. Our study clearly defines the APLN pathway as a central node in the pathogenesis of AAAs and the therapeutic strategy of enhancing the APLN pathway in treating AA. Enhancing APLN improves metabolic function and prevents sarcopenia and aging-related loss in muscle function (8), protects the failing heart (9, 32, 33) and pulmonary vasculature in patients with pulmonary arterial hypertension (7), and, as such, APLN analogs may confer unique therapeutic effects beyond AAAs.

Materials and Methods

All animal experiments were carried out in accordance with the Canadian Council on Animal Care Guidelines, and animal protocols were reviewed and approved by the Animal Care and Use Committee at the University of Alberta. Diseased and nondiseased human abdominal aortic specimens were collected at the University of Rochester, NY. Written consent was obtained from all participants, and our study was approved by the University of Rochester, Research Subjects Review Board. Ascending thoracic aorta from patients with bicuspid aortic valve, aortic dilation, and nondiseased aorta were collected as described before (34, 35). Materials and experimental procedures for animal models and protocols, peptide analysis and metabolism, RNA isolation, Taqman PCR, cell culture, tissue and cellular staining and immunofluorescence, flow cytometry, ultrasonic vasculography, vascular myography, blood pressure measurement, computer modeling, receptor binding, protein isolation, Western blotting, and quantification and statistical analysis are described in *SI Appendix, SI Materials and Methods*.

ACKNOWLEDGMENTS. This study was supported by an operating grant from the Canadian Institute for Advanced Research-Molecular Architecture of Life Program (CIHR, Grant 136921) to J.C.V., Canadian Institute for Health Research (CIHR, Grant PJT153306) to Z.K., HSF to G.Y.O. (Grant 855632).

1. K. C. Kent, Clinical practice. Abdominal aortic aneurysms. *N. Engl. J. Med.* **371**, 2101–2108 (2014).
2. X. Li, G. Zhao, J. Zhang, Z. Duan, S. Xin, Prevalence and trends of the abdominal aortic aneurysms epidemic in general populationA meta-analysis. *PLoS One* **8**, e81260 (2013).
3. M. E. Lindsay, H. C. Dietz, Lessons on the pathogenesis of aneurysm from heritable conditions. *Nature* **473**, 308–316 (2011).
4. D. Mozaffarian *et al.*; American Heart Association Statistics Committee and Stroke Statistics Subcommittee, Heart disease and stroke statistics–2015 update: A report from the American heart association. *Circulation* **131**, e29–e322 (2015).
5. V. B. Patel, J. C. Zhong, M. B. Grant, G. Y. Oudit, Role of the ACE2/angiotensin 1-7 axis of the renin-angiotensin system in heart failure. *Circ. Res.* **118**, 1313–1326 (2016).
6. W. Wang *et al.*, Loss of apelin exacerbates myocardial infarction adverse remodeling and ischemia-reperfusion injury: Therapeutic potential of synthetic apelin analogues. *J. Am. Heart Assoc.* **2**, e000249 (2013).
7. L. Brash *et al.*, Short-term hemodynamic effects of Apelin in patients with pulmonary arterial hypertension. *JACC Basic Transl. Sci.* **3**, 176–186 (2018).
8. C. Vinel *et al.*, The exerkine apelin reverses age-associated sarcopenia. *Nat. Med.* **24**, 1360–1371 (2018).
9. M. C. Scimia *et al.*, APJ acts as a dual receptor in cardiac hypertrophy. *Nature* **488**, 394–398 (2012).
10. H. J. Chun *et al.*, Apelin signaling antagonizes Ang II effects in mouse models of atherosclerosis. *J. Clin. Invest.* **118**, 3343–3354 (2008).
11. J. C. Zhong *et al.*, Apelin modulates aortic vascular tone via endothelial nitric oxide synthase phosphorylation pathway in diabetic mice. *Cardiovasc. Res.* **74**, 388–395 (2007).
12. Q. Liu *et al.*, Genetic targeting of sprouting angiogenesis using Apln-CreER. *Nat. Commun.* **6**, 6020 (2015).
13. N. De Mota *et al.*, Apelin, a potent diuretic neuropeptide counteracting vasopressin actions through inhibition of vasopressin neuron activity and vasopressin release. *Proc. Natl. Acad. Sci. U.S.A.* **101**, 10464–10469 (2004).
14. S. L. Pitkin, J. J. Maguire, T. I. Bonner, A. P. Davenport, International Union of Basic and Clinical Pharmacology. LXXIV. Apelin receptor nomenclature, distribution, pharmacology, and function. *Pharmacol. Rev.* **62**, 331–342 (2010).
15. V. B. Patel *et al.*, Loss of angiotensin-converting enzyme-2 exacerbates diabetic cardiovascular complications and leads to systolic and vascular dysfunction: A critical role of the angiotensin II/AT1 receptor axis. *Circ. Res.* **110**, 1322–1335 (2012).
16. J. Zhong *et al.*, Angiotensin-converting enzyme 2 suppresses pathological hypertrophy, myocardial fibrosis, and cardiac dysfunction. *Circulation* **122**, 717–728, (2010).

17. M. Haschke *et al*., Pharmacokinetics and pharmacodynamics of recombinant human angiotensin-converting enzyme 2 in healthy human subjects. *Clin. Pharmacokinet.* **52**, 783–792 (2013).
18. R. Basu *et al*., Loss of Timp3 gene leads to abdominal aortic aneurysm formation in response to angiotensin II. *J. Biol. Chem.* **287**, 44083–44096 (2012).
19. M. Shen *et al*., Divergent roles of matrix metalloproteinase 2 in pathogenesis of thoracic aortic aneurysm. *Arterioscler. Thromb. Vasc. Biol.* **35**, 888–898 (2015).
20. A. G. Bick *et al*., Cardiovascular homeostasis dependence on MICU2, a regulatory subunit of the mitochondrial calcium uniporter. *Proc. Natl. Acad. Sci. U.S.A.* **114**, E9096–E9104 (2017).
21. L. A. Cassis *et al*., ANG II infusion promotes abdominal aortic aneurysms independent of increased blood pressure in hypercholesterolemic mice. *Am. J. Physiol. Heart Circ. Physiol.* **296**, H1660–H1665 (2009).
22. S. M. McKinnie *et al*., The metalloprotease neprilysin degrades and inactivates apelin peptides. *Chembiochem* **17**, 1495–1498 (2016).
23. S. M. K. McKinnie *et al*., Synthetic modification within the "RPRL" region of apelin peptides: Impact on cardiovascular activity and stability to neprilysin and plasma degradation. *J. Med. Chem.* **60**, 6408–6427 (2017).
24. W. Wang *et al*., Angiotensin-converting enzyme 2 metabolizes and partially inactivates pyr-apelin-13 and apelin-17: Physiological effects in the cardiovascular system. *Hypertension* **68**, 365–377 (2016).
25. C. Fischer *et al*., Plasma kallikrein cleaves and inactivates apelin-17: Palmitoyl- and PEG-extended apelin-17 analogs as metabolically stable blood pressure-lowering agents. *Eur. J. Med. Chem.* **166**, 119–124 (2019).
26. A. M. O'Carroll, S. J. Lolait, L. E. Harris, G. R. Pope, The apelin receptor APJ: Journey from an orphan to a multifaceted regulator of homeostasis. *J. Endocrinol.* **219**, R13–R35 (2013).
27. C. Bernal-Mizrachi *et al*., Dexamethasone induction of hypertension and diabetes is PPAR-alpha dependent in LDL receptor-null mice. *Nat. Med.* **9**, 1069–1075 (2003).
28. B. T. Baxter, M. C. Terrin, R. L. Dalman, Medical management of small abdominal aortic aneurysms. *Circulation* **117**, 1883–1889 (2008).
29. M. Shen, M. Hu, P. W. M. Fedak, G. Y. Oudit, Z. Kassiri, Cell-specific functions of ADAM17 regulate the progression of thoracic aortic aneurysm. *Circ. Res.* **123**, 372–388 (2018).
30. R. Basu *et al*., Roles of angiotensin peptides and recombinant human ACE2 in heart failure. *J. Am. Coll. Cardiol.* **69**, 805–819 (2017).
31. B. Masri, N. Morin, L. Pedebernade, B. Knibiehler, Y. Audigier, The apelin receptor is coupled to Gi1 or Gi2 protein and is differentially desensitized by apelin fragments. *J. Biol. Chem.* **281**, 18317–18326 (2006).
32. Z. Z. Zhang *et al*., Apelin is a negative regulator of angiotensin II-mediated adverse myocardial remodeling and dysfunction. *Hypertension* **70**, 1165–1175 (2017).
33. A. G. Japp *et al*., Acute cardiovascular effects of apelin in humans: Potential role in patients with chronic heart failure. *Circulation* **121**, 1818–1827 (2010).
34. J. Lee *et al*., Gender-dependent aortic remodelling in patients with bicuspid aortic valve-associated thoracic aortic aneurysm. *J. Mol. Med. (Berl.)* **92**, 939–949 (2014).
35. V. B. Patel *et al*., Angiotensin-converting enzyme 2 is a critical determinant of angiotensin II-induced loss of vascular smooth muscle cells and adverse vascular remodeling. *Hypertension* **64**, 157–164 (2014).